International Review of Financial Analysis 84 (2022) 102324

Contents lists available at ScienceDirect

International Review of Financial Analysis

journal homepage: www.elsevier.com/locate/irfa

Multiscaling and rough volatility: An empirical investigation

Giuseppe Brandi [a,*], T. Di Matteo [a,b,c]

[a] Department of Mathematics, King's College London, WC2R 2LS London, UK
[b] Complexity Science Hub Vienna, 1080 Vienna, Austria
[c] Centro Ricerche Enrico Fermi, Via Panisperna 89 A, 00184 Rome, Italy

ARTICLE INFO

Keywords:
Rough volatility
Multiscaling
Time series
Robust correlation

ABSTRACT

Pricing derivatives goes back to the acclaimed Black and Scholes model. However, such a modelling approach is known not to be able to reproduce some of the financial stylised facts, including the dynamics of volatility. In the mathematical finance community, it has therefore emerged a new paradigm, named rough volatility modelling, that represents the volatility dynamics of financial assets as a fractional Brownian motion with Hurst exponent very small, which indeed produces rough paths. At the same time, prices' time series have been shown to be multiscaling, characterised by different Hurst scaling exponents. This paper assesses the interplay, if present, between price multiscaling and volatility roughness, defined as the (low) Hurst exponent of the volatility process. In particular, we perform extensive simulation experiments by using one of the leading rough volatility models present in the literature, the rough Bergomi model. A real data analysis is also conducted to test if the rough volatility model reproduces the same relationship. We find that the model can reproduce multiscaling features of the prices' time series when a low value of the Hurst exponent is used, but it fails to reproduce what the real data says. Indeed, we find that the dependency between prices' multiscaling and the Hurst exponent of the volatility process is diametrically opposite to what we find in real data, namely a negative interplay between the two.

1. Introduction

The history of derivatives pricing goes back to the famous Black and Scholes model (Black & Scholes, 1973; Merton, 1973). In the literature, several models added robustness to this original model by trying to adapt it more to reality. In particular, some models have introduced the direct modelling of the volatility dynamics of the diffusive price process (Heston, 1993). This modelling approach has the advantage of incorporating the dynamics of the volatility in the pricing procedure, avoiding the strong assumption of constant volatility. Moreover, in order to accommodate the stylised facts for which the volatility and price dynamics are empirically negatively dependent, a correlation parameter has been introduced between the Brownian motion that drives the two dynamics (Heston, 1993). Still, these features are not able to depict some aspects of the empirical data, i.e. the implied volatility surface (Bayer et al., 2016; Gatheral et al., 2018). For this reason, Gatheral et al. (2018) has introduced the concept of rough volatility. In this setting, the volatility dynamics is depicted as a fractional process (a fractional Brownian motion) with a very small Hurst exponent (the long-memory parameter). This is supported by the empirical analysis of Realised Variance (RV) measures[1] estimated by using high-frequency data. Several papers have reported that the realised variance has a value of the Hurst parameter very small, i.e. $H \sim 0.1$, i.e. volatility is rough (Bayer et al., 2016, 2019; Fukasawa et al., 2019; Gatheral et al., 2018; Takaishi, 2020). This new formulation is able to reproduce implied volatility surface dynamics more accurately.

However, in all these models, the stochastic process that drives the price dynamics is a standard Brownian motion, i.e. a process with Hurst parameter equal to 0.5. Indeed, log prices have been empirically shown to deviate from the Brownian motion paradigm in two main aspects. First, the long-memory parameter, the Hurst exponent, is not (statistically) equal to 0.5, and second, in contrast with the Brownian motion, different statistical moments yield different Hurst exponents, i.e. financial time series are multiscaling. The deviation from the Brownian motion paradigm can lead to arbitrage opportunities (Bender et al., 2007; Cheridito, 2003). However, as reported in various papers (Antoniades et al., 2021; Carbone et al., 2004; Grech & Pamuła, 2008; Kristoufek, 2010; Morales et al., 2012), the scaling exponents, when computed dynamically, are fluctuating and therefore difficult

* Corresponding author.
E-mail address: giuseppe.brandi@kcl.ac.uk (G. Brandi).

[1] Realised variance is the sum of squared returns over a specific time window for a specific time frequency. For example, the RV can be the sum of squared intra-day returns at 10 min frequency, which is an estimate of price variation over the day.

https://doi.org/10.1016/j.irfa.2022.102324
Received 25 January 2022; Received in revised form 3 July 2022; Accepted 28 July 2022
Available online 4 August 2022

to predict, making arbitrage strategies unreliable. Multiscaling is by now identified as stylised facts in financial time series. The study of scaling and multiscaling has been a prominent topic in the quantitative finance literature, which devoted most of the attention to financial time series to understand the source of multiscaling from an empirical and theoretical point of view (Buonocore et al., 2019; Calvet & Fisher, 2002; Di Matteo, 2007; Di Matteo et al., 2005; Gençay et al., 2001; Lux, 2004; Lux & Marchesi, 1999; Mandelbrot, 1963, 1967, 1971, 1972; Mantegna & Stanley, 1995). The estimation of multiscaling properties is challenging, and it requires robust statistical procedures (Brandi & Di Matteo, 2021).

Both multiscaling and rough volatility have been understood to originate from one or more phenomena related to trading dynamics. Still, unlike the analysis of the prices-volatility dependence, which has been shown to be strongly negative, to our knowledge, no dependency analysis of their scaling properties' has been produced so far. In particular, an important point is to investigate if rough volatility models are able to produce the multiscaling features empirically found in price time series and to study their interplay with volatility roughness (defined as the Hurst exponent of the volatility process). This might have substantial implications for modelling price behaviours and risk forecasting since by calibrating a wrong interplay, the degree of multiscaling in the price process would be under- or over-estimated.

In this paper, we fill this gap by studying the dependency between rough volatility and prices' multiscaling by using one of the benchmark rough volatility models, namely the rough Bergomi model (Bayer et al., 2016), and check if it is able to reproduce multiscaling and the same scaling structure of the real data. To this end, we first compute the Hurst exponent of the volatility process and the multiscaling measure of the price time series by using the methodology proposed in Brandi and Di Matteo (2021) and then compute a set of correlation coefficients between the two measures. We also use an outlier-robust correlation estimation methodology to check if results are affected by outliers (Pernet et al., 2013; Wilcox, 2004, 2011; Wilcox et al., 2018). The paper is structured as follows. Sections 2 and 3 review some concepts of fractional Brownian motion and rough volatility. Section 4 reports the statistical procedures used to estimate multiscaling and the correlation analysis. Section 5 shows the results of a simulation experiment by using the rough Bergomi model, while Section 6 those of the dependency analysis between prices' multiscaling and volatility roughness for real data. Section 7 concludes.

2. Fractional Brownian motion

Historically, the Black–Scholes (BS) model for option pricing (Black & Scholes, 1973; Merton, 1973) has been (and still is) the cornerstone in quantitative finance. By means of the Geometric Brownian motion, the authors provided an equation that can be used to compute the price of vanilla options. However, some researchers questioned the BS model's assumptions (Mandelbrot, 1967). In particular, one of these assumptions is the adoption of a Brownian motion for the price fluctuations, which implies no memory (Markovian property). A possible solution to this inconsistency with respect to the real data was identified by replacing the Brownian motion with a fractional Brownian motion (Mandelbrot, 1967; Mandelbrot & Wallis, 1968). A fractional Brownian motion is a stochastic process characterised by the following three properties (Taqqu, 2013):

(1) the process is Gaussian with zero mean;
(2) it has stationary increments;
(3) it is self-similar with index H, $0 < H < 1$.[2]

Fractional Brownian motion reduces to Brownian motion when $H = 1/2$, but in contrast to Brownian motion, it has dependent increments when $H \neq 1/2$, i.e. it is a non-Markovian process.[3] To compute the Hurst exponent from sample data, in this paper, we use the method of Brandi and Di Matteo (2021) that is based on the Generalised Hurst Exponent method (GHE) (see Antoniades et al., 2021; Buonocore et al., 2016, 2017; Di Matteo, 2007; Di Matteo et al., 2003, 2005; Kantelhardt et al., 2002). This methodology relies on the measurement of the direct scaling of the qth-order moments of the distribution of the increments (described in Section 4).[4] The GHE methodology returns the scaling exponent H_q. The most relevant (and used) values of q to assess the scaling properties of a time series are $q = 1$ and $q = 2$. The first one depicts the scaling of the absolute values of the increments and is closely related to the Hurst exponent originally proposed by Hurst (1956) while the second is associated with the scaling of the autocorrelation function of the process (Di Matteo, 2007). In the remainder of the paper, when not specified differently, we refer to H as the Hurst exponent computed for $q = 1$.

3. Rough volatility

Building on the work of Gatheral et al. (2018) on the statistical analysis of realised variance, rough volatility became a new paradigm in quantitative finance. It has been shown that realised variance (a proxy for rough volatility) is characterised by a process rougher that Brownian motion, i.e. $H < \frac{1}{2}$. This empirical observation led to the construction of stochastic models with strong anti-persistent volatility dynamics, the so-called rough volatility models (Fukasawa et al., 2019; Gatheral et al., 2018; Livieri et al., 2018; Takaishi, 2020). One of the leading models in this category is the rough Bergomi model (hereafter rBergomi) (see Bayer et al., 2016, 2019). In the rBergomi model, the dynamics for the asset price process S_t and the instantaneous variance process v_t are given by

$$\frac{\mathrm{d}S_t}{S_t} = \sqrt{v_t}\mathrm{d}\left(\lambda W_t + \sqrt{1-\lambda^2}W_t^{\perp}\right) \tag{1}$$

$$v_t = \xi_0(t)\exp\left(\eta W_t^H - \frac{1}{2}\eta^2 t^{2H}\right), \quad t \in [0,T]. \tag{2}$$

Here W_t and $W_t^{\perp}$ are two independent Brownian motions, T is the final time step, $\lambda \in [-1,1]$ is the correlation parameter between the price and volatility dynamics, $\eta > 0$ denotes the volatility of the volatility process, and $\xi_0(t)$ is the initial forward variance curve and H is the Hurst exponent. Moreover, W^H is a fractional Brownian motion given by

$$W_t^H = \sqrt{2H}\int_0^t (t-s)^{H-\frac{1}{2}}\mathrm{d}W_s, \quad t \in [0,T], \tag{3}$$

with the Hurst parameter being $H \in (0,1)$. Generally, rough volatility models are calibrated for H to be very small, i.e. $H \sim 0.1$. Due to the lack of Markovianity, conventional analytical pricing methods cannot be employed and Monte Carlo pricing methods based on simulated paths are used instead (McCrickerd & Pakkanen, 2018).

4. Multiscaling

In Section 2, we have recalled the fractional Brownian motion and the estimation of the Hurst exponent. However, financial time series have been shown to be not only scaling but also multiscaling (Di Matteo, 2007). To detect multiscaling, it is necessary to study the non-linearity of the scaling exponents of the q-order moments of the absolute value of the process increments (Calvet et al., 1997;

[2] The letter H denotes the original Hurst exponent, as in Mandelbrot and Van Ness (1968).

[3] Pricing derivatives under non-Markovianity is very challenging, and Monte-Carlo procedures are usually employed.

[4] For fractional Brownian processes, $H_q = H$ for all values of q.

Di Matteo, 2007; Mandelbrot et al., 1997). In particular, for a process $X(t)$ with stationary increments (at time aggregation τ) $r_\tau(t)$, i.e. $r_\tau(t) = X(t+\tau) - X(t)$, the GHE methodology considers a function of increments (Di Matteo, 2007) of the form

$$\Xi(\tau, q) = \mathbb{E}\left[|r_\tau(t)|^q\right] \sim K_q \tau^{qH_q}, \tag{4}$$

where $q = \{q_1, q_2, \dots, q_M\}$ is the set of evaluated moments, $\tau = \{\tau_1, \tau_2, \dots, \tau_N\}$ is the set of time aggregations used to compute the log-returns, N and M are the maximum numbers of moments and time aggregation' specifications, i.e. $q_1 = q_{min}$, $q_M = q_{max}$, $\tau_1 = \tau_{min}$ and $\tau_N = \tau_{max}$, K_q is the q-moment for $\tau = 1$, and H_q is the so called generalised Hurst exponent which is a function of q. Recently Brandi and Di Matteo (2021) proposed to compute the value of K_q by evaluating $\Xi(1, q)$ rather than estimating it via regression in order to remove any possible bias introduced in the estimation. By normalising the structure function $\Xi(\tau, q)$ as

$$\widetilde{\Xi}(\tau, q) = \frac{\Xi(\tau, q)}{K_q}, \tag{5}$$

Eq. (5) eliminates the possible bias introduced by the estimation of K_q via regression. Further, the q-order normalised moment is defined as

$$\ddot{\Xi}(\tau, q) = \widetilde{\Xi}(\tau, q)^{\frac{1}{q}} \tag{6}$$

from which follows that Eq. (4) becomes

$$\ddot{\Xi}(\tau, q) \sim \tau^{H_q}. \tag{7}$$

Within this new formulation, the q regressions have a 0 intercept and the multiscaling is present only if the regression coefficients H_q differ for distinct values of q. To assess multiscaling, it is then possible to analyze the equation of the form

$$H_q = A + Bq, \tag{8}$$

where A is the linear scaling index while B is the multiscaling proxy. In this mathematical setting, as for different multifractal models in finance (Bacry et al., 2001; Calvet & Fisher, 2002, 2004; Jiang et al., 2019), we implicitly assume a quadratic function of qH_q. Eliminating the multiplication by q from both sides of Eq. (8), we reduce the possibility of spurious results in case q is a dominant factor in the multiplication. By estimating B and testing its statistical significance, we are statistically able to identify multiscaling time series. In the following, we will refer to the scaling measures of the volatility process with the superscript (v) and with the superscript (P) for the prices, e.g. $H^{(v)}$, $B^{(v)}$, $H^{(P)}$ and $B^{(P)}$.

4.1. The choice of τ_{max}

As reported in Brandi and Di Matteo (2021), the choice of the maximum aggregation time is pivotal for the correct estimation of the scaling exponents and, by consequence, the multiscaling properties. This pivotal choice is mainly because in real data, even for very persistent time series, there is an aggregation cutoff from which the financial time series behave as uncorrelated. If we choose the maximum value of the aggregation time arbitrarily, we could mix a long-range correlation with an uncorrelated state, producing an erroneous estimation of the scaling exponents. To this extent, several methodologies have been proposed in the literature (Jiang et al., 2019). In this paper, we use the Autocorrelation Segmented Regression proposed in Brandi and Di Matteo (2021). The idea of this approach is to perform a segmented regression on the autocorrelation (or the autocovariance) function computed on the absolute returns and take $\tau_{max} = \tau^*$ as the splitting point between the long-range dependence state and the random state, which minimises the sum of squared residuals. By using the Autocorrelation Segmented Regression (ACSR), we can write the autocorrelation function of the absolute returns $r_\tau(t)$ for lag τ, $\phi_\tau(|r_\tau(t)|)$ as:

$$\phi_\tau(|r_\tau(t)|) = \begin{cases} \alpha + \tau^\beta, & \text{if } \tau < \tau_* \\ \alpha + \tau_*^\beta, & \text{if } \tau \geq \tau_* \end{cases} \tag{9}$$

where α is the intercept of the regression and that can be fixed to be equal to ϕ_1, β is a memory exponent for the autocorrelation function, τ is the lag at which the autocorrelation is computed, and $\hat{\tau}^*$ is the estimated value of aggregation which split the autocorrelation function between the correlated and random states. This estimated parameter will be used as τ_{max} in the GHE estimation procedure.

4.2. Analysis of dependence

In this paper, we are interested in analyzing the dependency between the scaling and multiscaling measures of the volatility time series and the scaling and multiscaling measures of the price process. Among the different measures available in the statistical literature, we use the Pearson and Spearman correlation coefficients. The Pearson correlation coefficient for any two random variables X and Y is defined as

$$\rho = \rho(X, Y) = \frac{Cov(X, Y)}{\sigma_X \sigma_Y}, \tag{10}$$

where Cov(X, Y) is the covariance between X and Y and σ_X and σ_X are the standard deviation of X and Y, respectively. Contrary to the Pearson correlation, the Spearman correlation captures the monotonic dependency (linear or nonlinear) between the two variables analyzed. Indeed, the Spearman correlation corresponds to the Pearson correlation between the rank values of the random variables. Let us define as $R(X)$ the ranks of X, the Spearman correlation is defined as:

$$\rho_S = \rho(R(X), R(Y)) = \frac{Cov(R(X), R(Y))}{\sigma_{R(X)} \sigma_{R(Y)}}, \tag{11}$$

where the quantities are defined as for the Pearson correlation.

5. The interplay between multiscaling and rough volatility: synthetic data

In this section, we simulate the rough Bergomi (rBergomi) model (Bayer et al., 2016, 2019) and check if it is able to produce multiscaling prices as recently demonstrated in Forde et al. (2022) for $H^{(v)} \to 0$. If it is the case, we want to understand what type of dependency structure there is between the model's parameters and the simulated prices multiscaling.[5] For the simulations, we use the parameters used in Bayer et al. (2016), i.e. $\eta = 1.9$, $\xi_0 = 0.1$ and varying values of the Hurst exponent H and correlation parameter λ in Eq. (1). We are interested in analyzing the model's potentiality to generate a dependency structure between the scaling measures of the two processes by changing the two parameters, H and λ. In particular, we set the correlation parameter λ to vary between -1 and $+1$ and the Hurst exponent H to vary between 0.01 and 0.99. To mimic the real data structure presented in Appendix B, and take into account any possible finite sample effect, for each combination of H and λ, we simulate 100 sets of time series (volatility and prices), each of which has been taken with the same lengths as the ones of the original dataset, i.e. $T = 5000$ time steps. We then compute $H^{(v)}$ and $B^{(P)}$ of the two simulated processes and analyze their dependence. Fig. 1 shows the impact of the Hurst parameter H and correlation parameter λ on the estimated multiscaling proxy B, $\hat{B}^{(P)}$.

Fig. 1 shows that the rBergomi model is indeed able to produce multiscaling prices for small values of H irrespective of the value of λ. Indeed, the effect of λ is very small and almost negligible. As it is possible to notice, the dependency relationship is stronger

[5] We report in Appendix A also the analysis done with respect to other scaling measures.

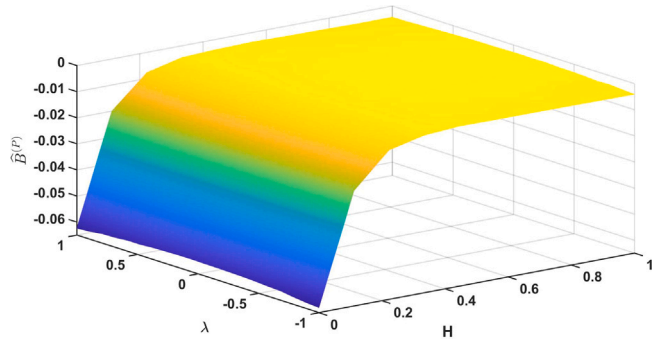

Fig. 1. Multiscaling proxy $\widehat{B}^{(P)}$ as a function of H and λ in the rBergomi model. The result is averaged over the 100 datasets and the plot is smoothed via interpolation for better representation.

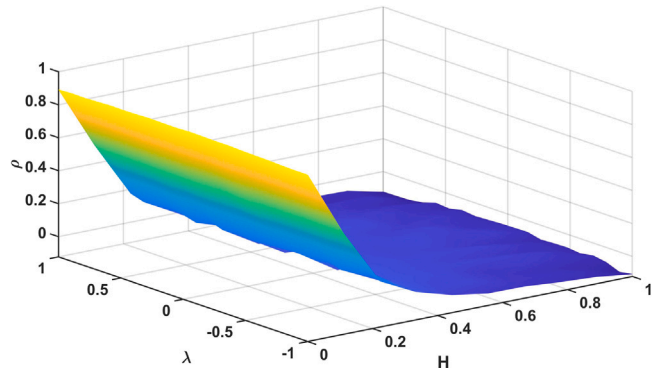

Fig. 2. Pearson correlation between Multiscaling proxy $\widehat{B}^{(P)}$ and $\widehat{H}^{(v)}$ as function of H and λ in the rBergomi model. The result is averaged over the 100 datasets and the plot is smoothed via interpolation for better representation.

for small values of H while it becomes negligible for high values of H. To numerically quantify this finding, we compute the Pearson and Spearman correlations between the volatility roughness $\widehat{H}^{(v)}$ and the price multiscaling $\widehat{B}^{(P)}$ for the 100 sets of time series. To better understand the local behavior of the dependency, we have partitioned the entire set of H values in 10 subsets with width 0.1, i.e. $\{(0, 0.01, \dots, 0.10), (0.10, 0.11, \dots, 0.20), \dots, (0.90, 0.91, \dots, 1)\}$ and we have computed the correlation coefficients between the estimated $H^{(v)}$ on each subset and the corresponding estimated values of the prices' multiscaling proxy $B^{(P)}$.[6] Results of the averaged Pearson correlations computed over the 100 simulated sets of times series are shown in Fig. 2.[7]

Fig. 2 confirms what was deduced from Fig. 1. The correlation between volatility roughness and price multiscaling diminishes as the Hurst exponent H of the volatility process increases. Furthermore, the correlation becomes negligible already for H near 0.3.[8] From this exploratory analysis, we might conclude that in order to retrieve both multiscaling and interplay between $\widehat{H}^{(v)}$ and $\widehat{B}^{(P)}$, we would need to use very low values of the Hurst exponent in Eq. (1), while the value of the parameter λ does not have a strong impact on the interplay.

[6] We repeated the same exercise with respect to λ, but we find an erratic behavior as λ does not play a significant role. For this reason, we do not report the plot.

[7] We report the same analysis with respect to the Spearman correlation in Fig. A.2 of Appendix A. The results are qualitatively equivalent to the Pearson correlation.

[8] The correlation for values equal or higher than 0.3 is not statistically significant at 5%.

6. The interplay between multiscaling and rough volatility: Real data

In the previous Section, we have shown that the rBergomi model is able to generate multiscaling prices when small values of H are used in Eq. (1), irrespective of the model's correlation parameter λ. We also found an overall nonlinear relationship between the level of multiscaling and the Hurst exponent H. In this section, we repeat a similar exercise as the one done in Section 5 and compute the correlation coefficients between the volatility roughness and price multiscaling of real data. This exercise allows us to understand if rough volatility models are in line with the empirical observations. In particular, by using data from the Oxford volatility library (Heber et al., 2009),[9] we first compute the Hurst exponent H on the realised variance (10 min frequency) time series, i.e. $\widehat{H}^{(v)}$ and the multiscaling proxy B on the prices time series, i.e, $\widehat{B}^{(P)}$. We then produce a set of correlation measures to quantify their interplay.[10]

6.1. Results

In this section, we report the procedure used on real data to compute the scaling exponents and the multiscaling proxy, defined as follows:

1. We first compute τ^* with the Autocorrelation Segmented Regression method introduced in Section 4.1 by using the absolute value of the open to close log-returns;[11]
2. We then perform the log–log regression of Eq. (7) for each index with $\tau_{max} = \widehat{\tau}^*$, that is the estimated τ^*.[12]
3. We finally compute the multiscaling proxy $\widehat{B}$ for each index by using Eq. (8) and test for its statistical significance.

Results of this procedure for the rough volatility measure (Realised Variance 10 min frequency) are reported in Table 1. A set of preliminary conclusions can be drawn from these results. First of all, it can be appreciated that there is heterogeneity in terms of optimal aggregation time even if many indices fall in the range between 1 and 3 trading years, with an average of 2 trading years. The second piece of evidence that can be extracted from Table 1 is that the volatility is indeed rough with a Hurst exponent ($\widehat{H}^{(v)}$ in the table) between ~ 0.08 and ~ 0.15 and that rough volatility presents very low (negligible) multiscaling values, as reported in other research papers (Gatheral et al., 2018; Livieri et al., 2018). In contrast to the realised variance time series, the prices time series present a much stronger multiscaling feature ($\widehat{B}^{(P)}$ in the table) across all markets, confirming what was found in a set of recent papers (Brandi & Di Matteo, 2021; Buonocore et al., 2019). Finally, it is possible to notice that apart from some cases, the Hurst exponent for prices is different from the 0.5 benchmark.[13]

After we computed the Hurst exponent of the realised variance time series and the multiscaling proxy of the prices time series and confirmed that prices are indeed multiscaling, we computed the correlation coefficients to measure their interplay. We find a negative correlation between $\widehat{H}^{(v)}$ and $\widehat{B}^{(P)}$ using both the Pearson and Spearman correlations. We found a Pearson correlation coefficient of -0.43 and a Spearman correlation coefficient of -0.51, both statistically significant at 5% level.

[9] Appendix B reports the description of the dataset.

[10] We also produced results for other scaling measures and different rough volatility proxies. Results are reported in Appendix C.

[11] Using close to close log-returns, the results remain qualitatively unchanged.

[12] We use $q_{min} = 0.05$ and $q_{max} = 1$ as prescribed in Brandi and Di Matteo (2021) and Buonocore et al. (2019).

[13] It is important to highlight the fact that being H an exponent, even small deviations from 0.5 are influential.

Table 1
Estimated maximum aggregation time, scaling, and multiscaling exponents for price and realised variance (at 10 min frequency) time series. Numbers in parenthesis represent the standard errors related to the estimated coefficients.

Index	τ_*	Prices		Volatility	
		$\widehat{H}^{(P)}$	$\widehat{B}^{(P)}$	$\widehat{H}^{(v)}$	$\widehat{B}^{(v)}$
AEX	516	0.5228 (0.0010)	−0.0273 (0.0001)	0.1302 (0.0016)	−0.0077 (0.0000)
AORD	507	0.5098 (0.0011)	−0.0038 (0.0001)	0.0605 (0.0016)	−0.0072 (0.0001)
BFX	446	0.5417 (0.0010)	−0.0323 (0.0002)	0.1360 (0.0016)	−0.0060 (0.0000)
BSESN	326	0.5346 (0.0013)	−0.0051 (0.0002)	0.1041 (0.0018)	−0.0066 (0.0000)
BVLG	461	0.4725 (0.0022)	−0.0227 (0.0001)	0.1069 (0.0027)	−0.0056 (0.0000)
BVSP	335	0.5042 (0.0010)	−0.0234 (0.0001)	0.1085 (0.0022)	−0.0041 (0.0000)
DJI	445	0.4786 (0.0011)	−0.0302 (0.0002)	0.1055 (0.0017)	−0.0053 (0.0001)
FCHI	578	0.4992 (0.0010)	−0.0322 (0.0001)	0.1227 (0.0016)	−0.0117 (0.0000)
FTMIB	256	0.4846 (0.0016)	−0.0264 (0.0000)	0.1119 (0.0027)	−0.0049 (0.0000)
FTSE	486	0.4854 (0.0012)	−0.0215 (0.0000)	0.1049 (0.0016)	−0.0094 (0.0001)
GDAXI	502	0.5188 (0.0010)	−0.0330 (0.0002)	0.1313 (0.0015)	−0.0114 (0.0000)
GSPTSE	337	0.5123 (0.0011)	−0.0222 (0.0000)	0.0915 (0.0019)	−0.0020 (0.0000)
HSI	669	0.5031 (0.0012)	−0.0236 (0.0001)	0.0825 (0.0018)	−0.0078 (0.0001)
IBEX	1070	0.5204 (0.0008)	−0.0296 (0.0000)	0.1369 (0.0012)	−0.0101 (0.0000)
IXIC	927	0.5289 (0.0011)	−0.0160 (0.0002)	0.1030 (0.0015)	−0.0088 (0.0000)
KS11	985	0.5092 (0.0010)	−0.0141 (0.0001)	0.0877 (0.0016)	−0.0074 (0.0000)
KSE	103	0.5823 (0.0017)	−0.0240 (0.0002)	0.1116 (0.0029)	−0.0000 (0.0006)
MXX	1096	0.5402 (0.0008)	−0.0392 (0.0002)	0.0749 (0.0016)	−0.0170 (0.0001)
N225	344	0.5174 (0.0009)	−0.0171 (0.0000)	0.0963 (0.0019)	−0.0032 (0.0000)
NSEI	477	0.5307 (0.0011)	−0.0138 (0.0001)	0.1041 (0.0015)	−0.0054 (0.0000)
OMXC20	439	0.5172 (0.0013)	−0.0200 (0.0002)	0.1036 (0.0021)	−0.0071 (0.0000)
OMXHPI	371	0.5143 (0.0012)	−0.0170 (0.0001)	0.1166 (0.0019)	−0.0077 (0.0000)
OMXSPI	444	0.5064 (0.0016)	−0.0153 (0.0000)	0.1238 (0.0018)	−0.0074 (0.0000)
OSEAX	332	0.5314 (0.0010)	−0.0138 (0.0001)	0.0933 (0.0017)	−0.0084 (0.0001)
RUT	229	0.4705 (0.0013)	−0.0054 (0.0000)	0.1100 (0.0020)	−0.0019 (0.0000)
SMSI	643	0.5232 (0.0011)	−0.0322 (0.0001)	0.1276 (0.0016)	−0.0121 (0.0001)
SPX	477	0.4962 (0.0011)	−0.0286 (0.0001)	0.1146 (0.0017)	−0.0018 (0.0000)
SSEC	511	0.5700 (0.0013)	−0.0197 (0.0001)	0.1141 (0.0017)	−0.0070 (0.0000)
SSMI	528	0.5097 (0.0010)	−0.0251 (0.0000)	0.1350 (0.0017)	−0.0040 (0.0000)
STI	598	0.5568 (0.0013)	−0.0177 (0.0001)	0.0724 (0.0023)	−0.0091 (0.0001)
STOXX50E	504	0.5043 (0.0010)	−0.0347 (0.0002)	0.1178 (0.0017)	−0.0191 (0.0000)

6.2. Robust correlation analysis

Although easy to implement, Eq. (10) is known to be strongly affected by outliers. In fact, even a very small portion of outliers can severely bias its estimated correlation coefficient. To tackle this issue, several methodologies have been proposed in the robust statistics literature. Some methodologies act at reducing the impact of the outliers by downweighting their contribution in the computation of the correlation coefficient. In contrast, other methods compute the correlation over the outliers-filtered dataset. In a set of papers (Pernet et al., 2013; Wilcox, 2004; Wilcox et al., 2018), it has been shown that the second approach gives better results in reducing the bias. For this reason, we compute the correlation coefficient on the outlier filtered dataset. In particular, we are interested in removing the multivariate outliers, which are the relevant ones for the computation of the correlation coefficient. To this extent, we employ the bivariate outliers detection method of Pernet et al. (2013).[14] From this analysis, we found out that IPC Mexico (MXX) is an outlier and for this reason, we label it as an outlier in our correlation analysis. We define the robust correlations as $\tilde{\rho}$ (or $\tilde{\rho_S}$), i.e. the correlation coefficient computed on the dataset without considering IPC Mexico (MXX). The results are depicted in Fig. 3, where we also report the correlation coefficients that have not been corrected for the outlier.

As we can observe from Fig. 3, the interplay between volatility roughness and prices' multiscaling is strongly negative. In fact, the rougher the volatility process is, the less multiscaling is the price time series. Indeed, it is much stronger than what the found in the simulation experiment (for similar values of H), and the dependency is in the opposite direction. This result highlights the fact that the rBergomi model cannot reproduce this strong empirical dependency structure. This result calls for the development of models which can accommodate both multiscaling prices and rough volatility and their negative correlation.

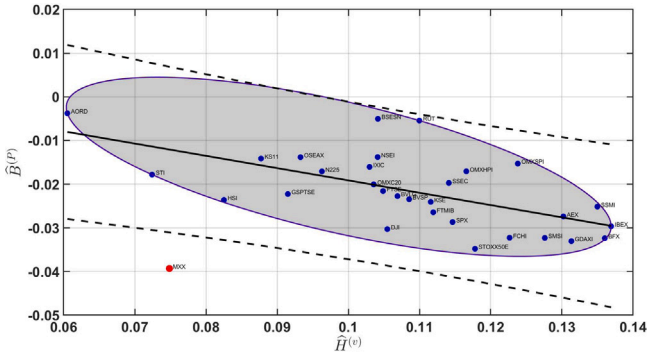

Fig. 3. Estimated multiscaling proxy of the prices $\widehat{B}^{(P)}$ as function of volatility roughness $\widehat{H}^{(v)}$ (realised variance at 10 min frequency). Blue dots label different indices, the black continuous line is the regression line, while the black dashed lines are the 95% confidence intervals. Pearson correlation coefficient ρ is −0.43 and Spearman correlation coefficient ρ_S is −0.51. The outlier-robust versions, $\tilde{\rho}$ and $\tilde{\rho}_S$ are equal to −0.61 and −0.65 respectively. All correlations are statistically significant at 5% level. (For interpretation of the references to color in this figure legend, the reader is referred to the web version of this article.)

Finally, to check if the result is dependent on the heterogeneity and distribution of the Hurst exponents $\widehat{H}^{(v)}$ of the real data and to the maximum time aggregation τ_{max} used for the estimation of the scaling exponents, we simulated 100 set of time series (prices and volatility) using the rBergomi model, each one composed by 31 time series with the specific set of $\widehat{H}^{(v)}$ estimated from the real data (see Table 1) and with a varying level of the correlation parameter λ (the remaining parameters are left unchanged). The estimation is then carried over by using the same procedure described in Section 6.1, by using the same τ_{max} of Table 1. Results are reported in Fig. 4, where we report both

[14] The entire procedure used to detect the outliers is reported in Appendix D.

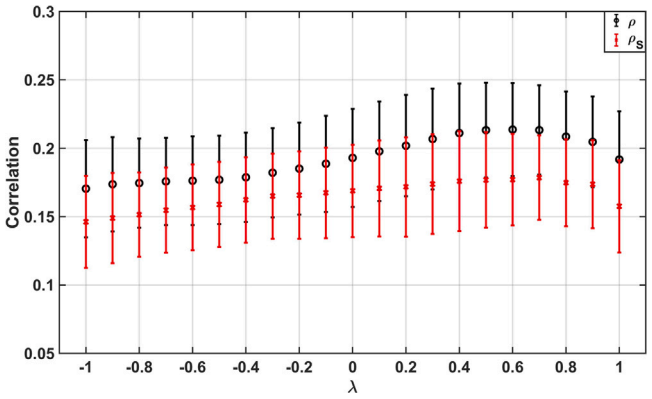

Fig. 4. Correlation coefficients between $\widehat{H}^{(v)}$ and $\widehat{B}^{(P)}$ as function of λ for the rBergomi model with H taken from Table 1, $\xi = 0.01$, $\eta = 1.9$. The black line is the Pearson correlation, while the red line corresponds to the Spearman correlation. Statistics computed over 100 simulations, each composed of 31 simulated paths each of 5000 time steps. The error bars represent the standard errors. The plot has been smoothed via interpolation for better representation. (For interpretation of the references to color in this figure legend, the reader is referred to the web version of this article.)

correlation measures as a function of λ.[15] As it is possible to observe, the correlation is positive for each value of λ with a peak near the positive boundary. This highlights the fact that it is not the heterogeneity of the true data that produced the result, which is indeed robust.

7. Summary and final remarks

To check for any interplay between prices' multiscaling and volatility roughness, we have produced extensive simulation experiments by using one of the benchmark models in the financial mathematics literature on rough volatility, namely the rough Bergomi model. By using the model parameters in Bayer et al. (2016, 2019) and by changing the Wiener processes correlation and the Hurst exponent, we have investigated if the simulated volatility and price processes showed any relationship in their scaling exponents. We have found that the correlation between prices' multiscaling and rough volatility is mainly positive, peaking for small values of H, while the correlation parameter λ does not play a major role in this relationship. We have then computed the same dependency measures by using real data. We have found that there exists a statistically significant (negative) dependence between volatility roughness and prices' multiscaling by analyzing different indices. In particular, we have found that the rougher the volatility is, the less multiscaling the price series are. This result shows that even if the rBergomi is able to produce multiscaling prices for low values of H, the empirical dependence is reversed. To check if the heterogeneity of the empirical scaling exponents was producing an artefact dependency structure, we have produced a new simulation experiment in which the scaling exponents of the volatility process were taken from the ones we have estimated from the real data. Even in this case, we found that the model is not able to reproduce the interplay found in the real data. This result shows that current models cannot reproduce this higher-order dependence between the scaling features of the volatility and price processes. Indeed, calibrating H in the volatility process would produce the opposite effect on the prices multiscaling, e.g. low H would imply higher multiscaling prices while it should generate prices with a low level of multiscaling. A possible solution to this is to employ multiscaling models for the price fluctuations and a fractional type of process for the volatility dynamics. In particular, it would be advisable to link the multiscaling measures of the prices' process with the volatility roughness. One possibility would be to implement a time-changed Brownian motion for the log-prices fluctuations, where the time change measure is indeed multifractal with the intermittency parameter linked to the Hurst exponent of the underlying volatility process. This will generate more reliable price time series that, combined with turbo-charged Monte Carlo procedures, McCrickerd and Pakkanen (2018) can be used to make forecasts and price Options. Future analysis might include the investigation of the dynamic dependency between the scaling measures in order to check for trends and cycles. Finally, since rough volatility is not directly observed but proxied by various measures (realised variance, for example), it would be beneficial to understand the impact of such volatility proxies on the dependency structure between price multiscaling and volatility roughness.

[15] Additional results related to the correlation between other scaling measures are reported in Appendix C.

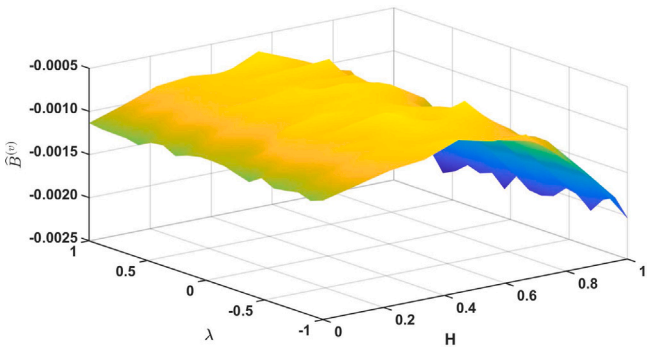

Fig. A.1. Multiscaling proxy $\widehat{B}^{(v)}$ with respect to H and λ in the rBergomi model. The result is averaged over the 100 dataset and the plot is smoothed via interpolation for better representation.

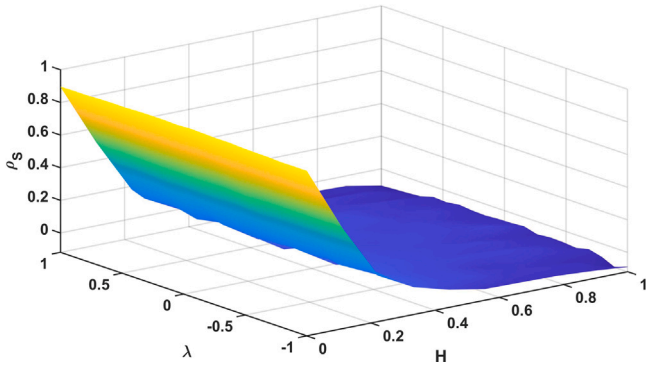

Fig. A.2. Spearman correlation ρ_S between the multiscaling proxy $\widehat{B}^{(P)}$ and $\widehat{H}^{(v)}$. Description as for caption of Fig. 2.

Declaration of competing interest

The authors declare that they have no known competing financial interests or personal relationships that could have appeared to influence the work reported in this paper.

Appendix A. Additional results: Synthetic data

In this Section, we report additional results related to the analysis of scaling exponents of both volatility and prices processes and their interplay related to the synthetic data.

As it is possible to see from Fig. A.1, even if the level of multiscaling increases with respect to H, it remains negligible also for $H \sim 1$.

As for the Pearson correlation of Fig. 2, we find that the Spearman correlation between the multiscaling proxy $\widehat{B}^{(P)}$ and $\widehat{H}^{(v)}$ is higher for small values of H and becomes negligible for $H > 0.3$.

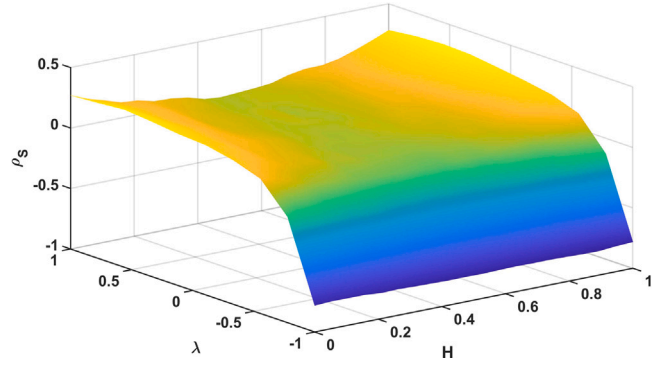

Fig. A.3. Spearman correlation between Multiscaling proxy $\widehat{H}^{(P)}$ and $\widehat{H}^{(v)}$. Description as for caption of Fig. 2.

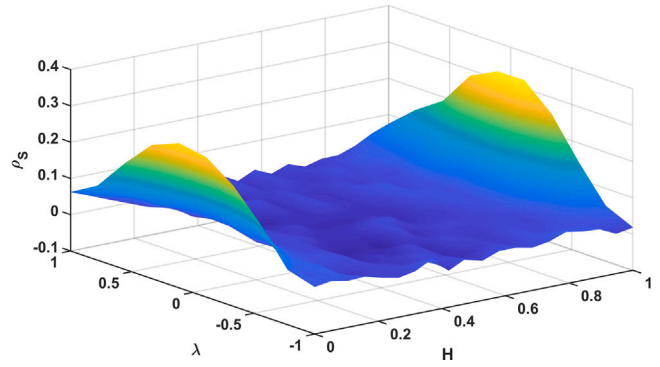

Fig. A.4. Spearman correlation between Multiscaling proxy $\widehat{B}^{(P)}$ and $\widehat{B}^{(v)}$. Description as for caption of Fig. 2.

For completeness, we also report the correlations between the Hurst exponent of the prices and volatility processes, as well as the dependence between their multiscaling features.

As we can observe from Fig. A.3, the correlation between the Hurst exponents of the two processes is almost entirely generated by the correlation parameter λ. This is not an unexpected result since the λ drives the correlation between the two processes' diffusive components.

With respect to the interplay between the multiscaling features of the two processes, there is a correlation at the boundaries of the parameter H (see Fig. A.4). This is due to the following motivation. As it is possible to see from Fig. 1, the slope of the prices' multiscaling proxy $\widehat{B}^{(P)}$ is strongly positive for $H \sim 0$, then it becomes flat for intermediate values of H. For high values of H, even if not statistically significant, it becomes slightly negative. The same type of behaviour, even if with a different strength, is reported in Fig. A.1 for the multiscaling feature of the volatility process. Indeed, the slope of the of $\widehat{B}^{(v)}$ for small values of H, even if not statistically significant, is positive, while it is negative for $H \sim 1$. For these reasons, the correlation between the multiscaling features of the two processes is positive at the boundaries of H. However, these correlations are not statistically significant at 5% level.

Appendix B. Data

The data used in this paper are taken from the Oxford volatility library (Heber et al., 2009). Codes and descriptions are reported in the Table B.1 while the stock indices available and the time periods for which the data are available are reported in Table B.2. The data is checked for missing values, and in the cases in which a datapoint is not available, a linear interpolation method is used to input the datum.

Table B.1
Variables of the Oxford Volatility Library used in the paper.

Code	Description
close_price	Closing (Last) Price
open_to_close	Open to Close log-Return
rv10	Realised Variance (10-min)
rv5	Realised Variance (5-min)
rsv	Realised Semi-variance (5-min)
bv	Bipower Variation (5-min)

Table B.2
Information of the Oxford volatility library dataset.

Index	Market name	First date	Last date
AEX	AEX index	03/01/2000	11/11/2021
AORD	All Ordinaries	04/01/2000	11/11/2021
BFX	Bell 20 Index	03/01/2000	11/11/2021
BSESN	S&P BSE Sensex	03/01/2000	11/11/2021
BVLG	PSI All-Share Index	15/10/2012	11/11/2021
BVSP	BVSP BOVESPA Index	03/01/2000	11/11/2021
DJI	Dow Jones Industrial Average	03/01/2000	11/11/2021
FCHI	CAC 40	03/01/2000	11/11/2021
FTMIB	FTSE MIB	01/06/2009	11/11/2021
FTSE	FTSE 100	04/01/2000	11/11/2021
GDAXI	DAX	03/01/2000	11/11/2021
GSPTSE	S&P/TSX Composite index	02/05/2002	11/11/2021
HSI	HANG SENG Index	03/01/2000	11/11/2021
IBEX	IBEX 35 Index	03/01/2000	11/11/2021
IXIC	Nasdaq 100	03/01/2000	11/11/2021
KS11	Korea Composite Stock Price Index	04/01/2000	11/11/2021
KSE	Karachi SE 100 Index	03/01/2000	11/11/2021
MXX	IPC Mexico	03/01/2000	11/11/2021
N225	Nikkei 225	02/02/2000	11/11/2021
NSEI	NIFTY 50	03/01/2000	11/11/2021
OMXC20	OMX Copenhagen 20 Index	03/10/2005	11/11/2021
OMXHPI	OMX Helsinki All Share Index	03/10/2005	11/11/2021
OMXSPI	OMX Stockholm All Share Index	03/10/2005	11/11/2021
OSEAX	Oslo Exchange All-share Index	03/09/2001	11/11/2021
RUT	Russel 2000	03/01/2000	11/11/2021
SMSI	Madrid General Index	04/07/2005	11/11/2021
SPX	S&P 500 Index	03/01/2000	11/11/2021
SSEC	Shanghai Composite Index	04/01/2000	11/11/2021
SSMI	Swiss Stock Market Index	04/01/2000	11/11/2021
STI	Straits Times Index	03/01/2000	11/11/2021
STOXX50E	EURO STOXX 50	03/01/2000	11/11/2021

close_price: Daily closing price. The closing price is the last observed price of the day.

open_to_close: Daily open to close returns are the log-returns computed between the opening price and the closing price for each day.

rv5 and rv10: Realised variance at 5 min and 10 min sampling frequency. These measures are computed as the sum of squared returns over a specific time window and a specific time frequency. For example, the RV can be the sum of squared intra-day returns at 10 min frequency.

rsv5: Realised semi-variance at 5 min sampling frequency. The realised semi-variance is calculated by first computing the realised variance for negative and positive returns separately and then summing them up.

bv: Realised Bipower Variation at 5 min sampling frequency. mn Bipower variation is computed as the (scaled) sum of products of adjacent absolute returns.

Appendix C. Additional results: Real data

In this section, we report the additional results related to the analysis of the real data. When computing the correlation over the real data scaling features, we report both the standard and robust measures of correlations.

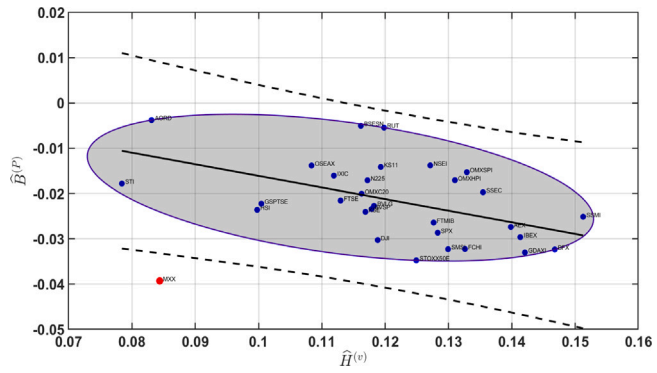

Fig. C.1. Estimated multiscaling proxy of the prices $\widehat{B}^{(P)}$ as function of volatility roughness $\widehat{H}^{(v)}$ (realised variance at 5 min frequency). Pearson correlation coefficient ρ is −0.30 and Spearman correlation coefficient ρ_S is −0.39. The outlier-robust versions, $\tilde{\rho}$ and $\tilde{\rho}_S$ are equal to −0.51 and −0.51 respectively. Description as in caption of Fig. 3.

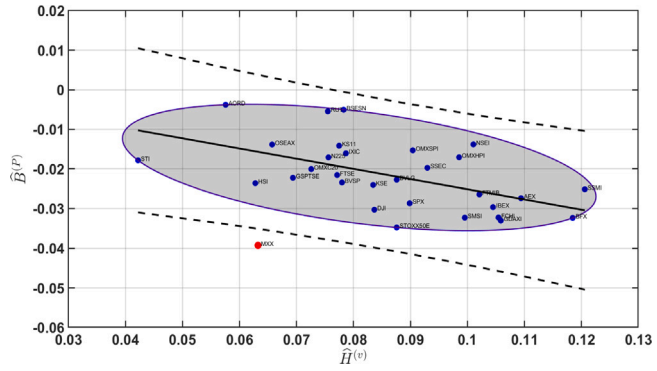

Fig. C.2. Estimated multiscaling proxy of the prices $\widehat{B}^{(P)}$ as function of volatility roughness $\widehat{H}^{(v)}$ (realised semi-variance at 5 min frequency). Pearson correlation coefficient ρ is −0.42 and Spearman correlation coefficient ρ_S is −0.45. The outlier-robust versions, $\tilde{\rho}$ and $\tilde{\rho}_S$ are equal to −0.55 and −0.57 respectively. Description as in caption of Fig. 3.

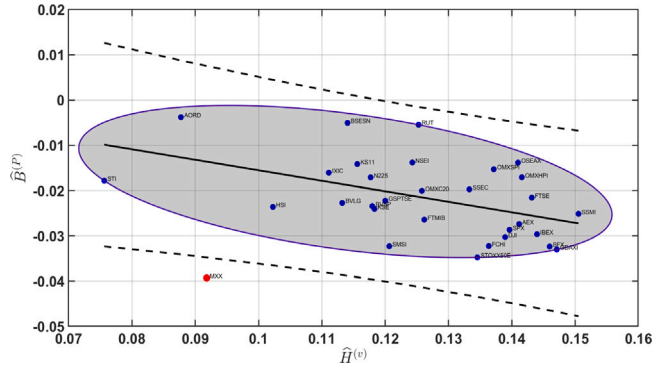

Fig. C.3. Estimated multiscaling proxy of the prices $\widehat{B}^{(P)}$ as function of volatility roughness $\widehat{H}^{(v)}$ (bipower variation at 5 min frequency). Pearson correlation coefficient ρ is −0.30 and Spearman correlation coefficient ρ_S is −0.36. The outlier-robust versions, $\tilde{\rho}$ and $\tilde{\rho}_S$ are equal to −0.48 and −0.48 respectively. Description as in caption of Fig. 3.

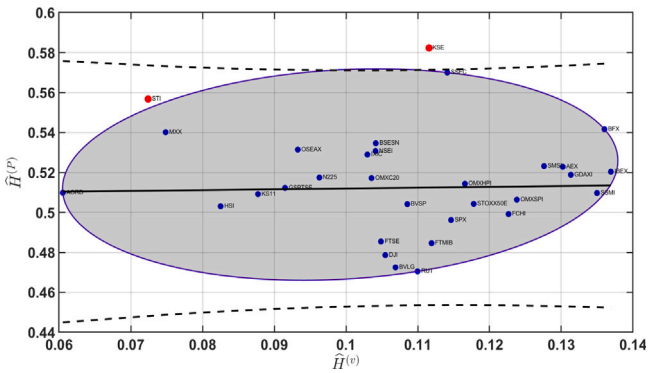

Fig. C.4. Estimated Hurst exponent of the prices $\widehat{H}^{(P)}$ as function of volatility roughness $\widehat{H}^{(v)}$ (realised variance at 10 min frequency). Pearson correlation coefficient ρ is −0.06 and Spearman correlation coefficient ρ_S is −0.06. The outlier-robust versions, $\tilde{\rho}$ and $\tilde{\rho}_S$ are equal to 0.03 and 0.00 respectively. Description as in caption of Fig. 3.

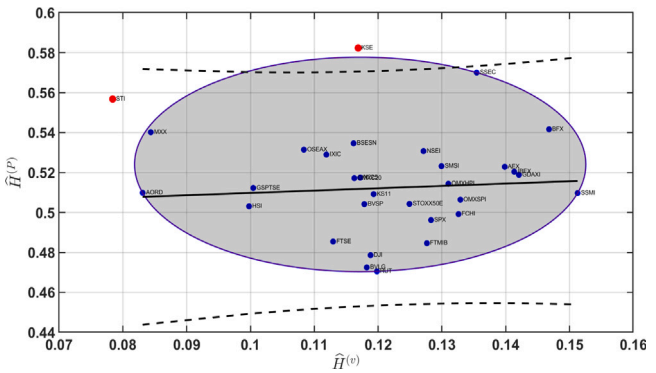

Fig. C.5. Estimated Hurst exponent of the prices $\widehat{H}^{(P)}$ as function of volatility roughness $\widehat{H}^{(v)}$ (realised variance at 5 min frequency). Pearson correlation coefficient ρ is −0.09 and Spearman correlation coefficient ρ_S is −0.06. The outlier-robust versions, $\tilde{\rho}$ and $\tilde{\rho}_S$ are equal to 0.09 and 0.08 respectively. Description as in caption of Fig. 3.

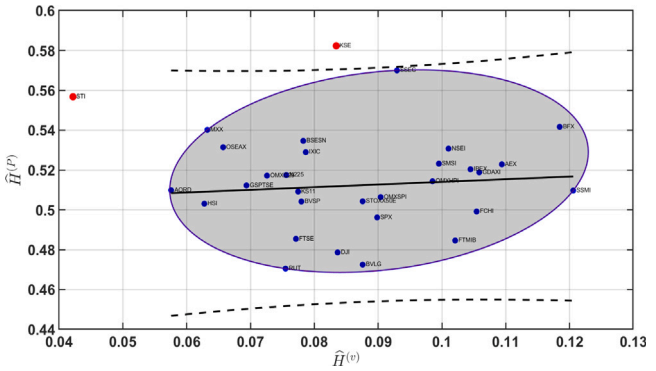

Fig. C.6. Estimated Hurst exponent of the prices $\widehat{H}^{(P)}$ as function of volatility roughness $\widehat{H}^{(v)}$ (realised semi-variance at 5 min frequency). Pearson correlation coefficient ρ is −0.07 and Spearman correlation coefficient ρ_S is 0.01. The outlier-robust versions, $\tilde{\rho}$ and $\tilde{\rho}_S$ are equal to 0.10 and 0.12 respectively. Description as in caption of Fig. 3.

C.1. Volatility roughness and price multiscaling

In this subsection, we report additional results related to different volatility measures with respect to the one presented in the main text (see Figs. C.1–C.3).

As we can see from the figures, the same pattern as for the realised variance at 10 min sampling frequency analyzed in the main text is retrieved for different rough volatility measures.

C.2. Volatility roughness and price scaling

In this subsection, we report additional results related to the study of the correlation between volatility roughness and price scaling for different volatility measures (see Figs. C.4–C.7).

As it is possible to notice from the plots of this section, there is no statistical relationship between the Hurst exponents of the volatility

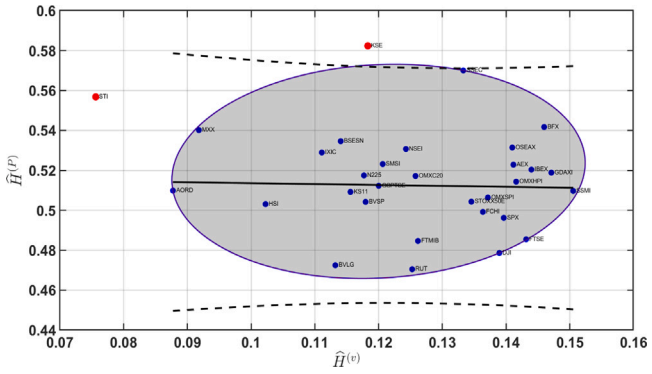

Fig. C.7. Estimated Hurst exponent of the prices $\widehat{H}^{(P)}$ as function of volatility roughness $\widehat{H}^{(v)}$ (bipower variation at 5 min frequency). Pearson correlation coefficient ρ is −0.21 and Spearman correlation coefficient ρ_S is −0.11. The outlier-robust versions, $\tilde{\rho}$ and $\tilde{\rho}_S$ are equal to −0.03 and 0.00 respectively. Description as in caption of Fig. 3.

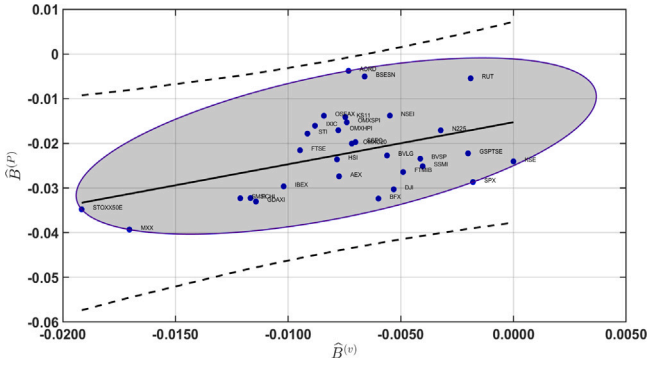

Fig. C.8. Estimated multiscaling proxy of the prices $\widehat{B}^{(P)}$ as function of volatility multiscaling $\widehat{B}^{(v)}$ (realised variance at 10 min frequency). Pearson correlation coefficient ρ is 0.44 and Spearman correlation coefficient ρ_S is 0.29. No outlier has been detected. Description as in caption of Fig. 3.

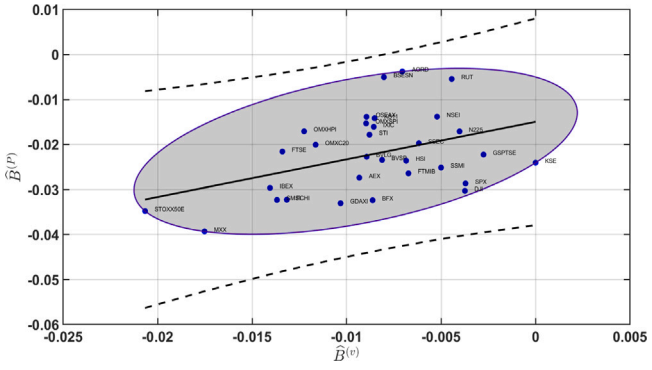

Fig. C.9. Estimated multiscaling proxy of the prices $\widehat{B}^{(P)}$ as function of volatility multiscaling $\widehat{B}^{(v)}$ (realised variance at 5 min frequency). Pearson correlation coefficient ρ is 0.41 and Spearman correlation coefficient ρ_S is 0.33. No outlier has been detected. Description as in caption of Fig. 3.

and prices time series. Indeed, all correlation coefficients are not statistically significant, and the robust correlation coefficients also confirm this result.

C.3. Volatility multiscaling and price multiscaling

In this subsection, we report additional results related to the study of the correlation between volatility multiscaling and price multiscaling for different volatility measures.

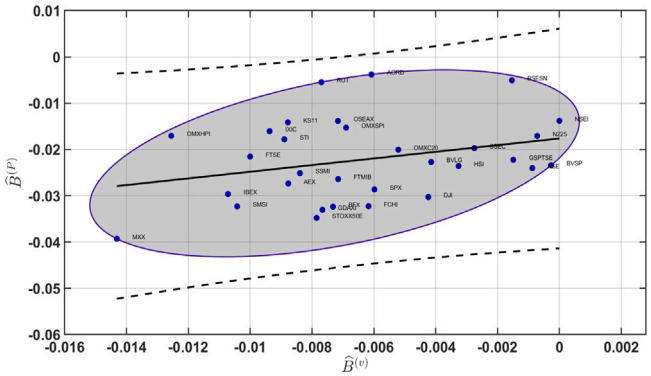

Fig. C.10. Estimated multiscaling proxy of the prices $\widehat{B}^{(P)}$ as function of volatility multiscaling $\widehat{B}^{(v)}$ (realised semi-variance at 5 min frequency). Pearson correlation coefficient ρ is 0.30 and Spearman correlation coefficient ρ_S is 0.25. No outlier has been detected. Description as in caption of Fig. 3.

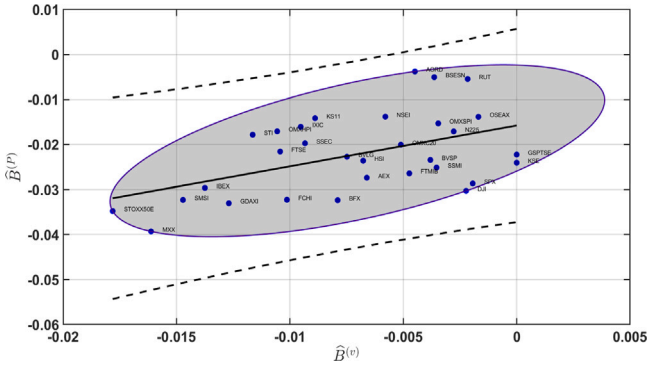

Fig. C.11. Estimated multiscaling proxy of the prices $\widehat{B}^{(P)}$ as function of volatility multiscaling $\widehat{B}^{(v)}$ (bipower variation at 5 min frequency). Pearson correlation coefficient ρ is 0.49 and Spearman correlation coefficient ρ_S is 0.40. No outlier has been detected. Description as in caption of Fig. 3.

Figs. C.8–C.11 show that the correlation between the multiscaling features of the volatility and price processes is positive. Furthermore, the Pearson correlation is statistically significant across different volatility measures, while the Spearman correlation is not statistically significant for all the volatility measures.

C.4. Simulated data with empirical hurst exponent

Fig. C.12 shows that the rBergomi produces a correlation between the Hurst exponents of the volatility and the Hurst exponent of the prices process, which is in line with the input correlation λ of the Brownian motions. Indeed, the correlation between $\widehat{H}^{(v)}$ and $\widehat{H}^{(P)}$ is not statistically significant at 5% for values of λ between −0.6 and 0.5. On the other hand, the correlation between the multiscaling features is stable around ∼0.18 irrespective of λ, confirming that λ does not have a direct effect on the multiscaling properties of volatility and prices processes (see Fig. C.13).

Appendix D. Outlier identification procedure

Let's $X \in \mathcal{R}^{N\times 2}$ be the bivariate dataset (in our case X is composed by $\widehat{H}^{(v)}$ and $\widehat{B}^{(P)}$) composed by N datapoints with indices $I \in \{1, \dots, N\}$. The procedure is as follow:

1. Compute the Minimum Covariance Determinant (MCD) of the dataset (Hubert et al., 2018)
2. Compute μ as the center of the data scatter cloud given by the MCD (Pernet et al., 2013)

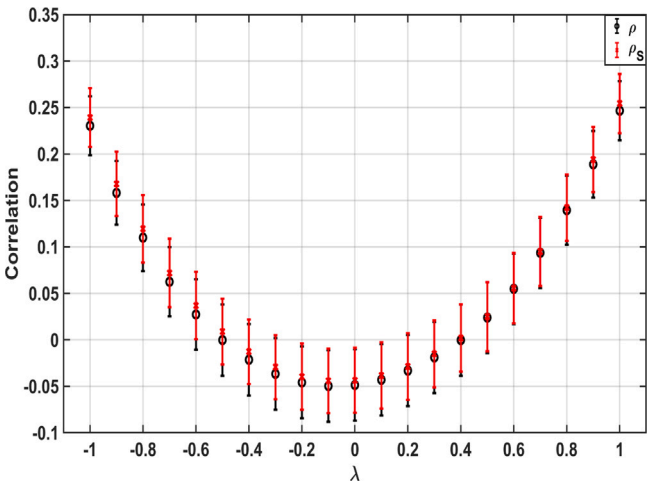

Fig. C.12. Correlation coefficients between $\widehat{H}^{(v)}$ and $\widehat{H}^{(P)}$ as function of λ for the rBergomi model with H taken from Table 1, $\xi = 0.01$, $\eta = 1.9$. Description as reported in caption of Fig. 4.

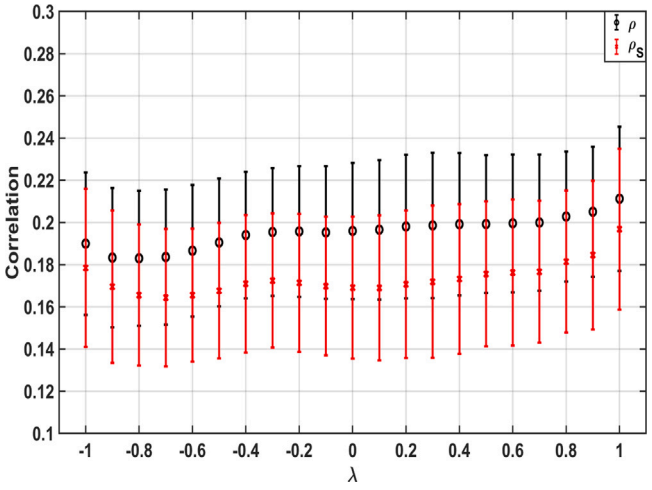

Fig. C.13. Correlation coefficients between $\widehat{B}^{(v)}$ and $\widehat{B}^{(P)}$ as function of λ for the rBergomi model with H taken from Table 1, $\xi = 0.01$, $\eta = 1.9$. Description as reported in the caption of Fig. 4.

3. Compute the (Euclidean) distance D_i to the center of the data, i.e. $X - \mu$ for all set of points $i = 1, \dots, N$
4. Use the (corrected) Boxplot rule by Carling (2000) to detect the outliers in D_i
5. Define the set of outliers as o and the set of datapoints without outliers as $I = I \setminus o$
6. Compute the robust correlation coefficient $\tilde{\rho} = \rho(X_I)$, where X_I is the set of bivariate datapoints filtered by outliers.

For the parameter choice in the various steps of the procedure, we use the optimal ones described in Carling (2000), Pernet et al. (2013) and Hubert et al. (2018). It is important to notice that being the MCD is a robust method to compute a scatter matrix (covariance matrix), a robust correlation coefficient can be computed directly from it Hubert et al. (2018).

Regarding the procedure used to detect outliers, it is possible that some bivariate datapoints are outliers for one specification (volatility measure) but not for another. In order to remove only the extreme outlier(s) which affect all the specifications, we define as the set of outliers the intersection between the outliers found across different volatility measures.[16] Define m as the index of a specific volatility measure. We define o_m as the set of outliers for a specific volatility measure m. The overall outlier set is computed as:

$$\tilde{o} = \bigcap_m o_m, \tag{D.1}$$

where $\tilde{o}$ is the set of outliers for all the specifications.

References

Antoniades, I., Brandi, G., Magafas, L., & Di Matteo, T. (2021). The use of scaling properties to detect relevant changes in financial time series: A new visual warning tool. *Physica A: Statistical Mechanics and its Applications*, *565*, Article 125561.

Bacry, E., Delour, J., & Muzy, J.-F. (2001). Multifractal random walk. *Physical Review E*, *64*(2), Article 026103.

Bayer, C., Friz, P., & Gatheral, J. (2016). Pricing under rough volatility. *Quantitative Finance*, *16*(6), 887–904.

Bayer, C., Horvath, B., Muguruza, A., Stemper, B., & Tomas, M. (2019). On deep calibration of (rough) stochastic volatility models. arXiv preprint arXiv:1908.08806.

Bender, C., Sottinen, T., & Valkeila, E. (2007). Arbitrage with fractional Brownian motion? *Theory of Stochastic Processes*, *13*(1), 23–34.

Black, F., & Scholes, M. (1973). The pricing of options and corporate liabilities. *Journal of Political Economy*, *81*(3), 637–654.

Brandi, G., & Di Matteo, T. (2021). On the statistics of scaling exponents and the multiscaling value at risk. *The European Journal of Finance*, 1–22.

Buonocore, R. J., Aste, T., & Di Matteo, T. (2016). Measuring multiscaling in financial time-series. *Chaos, Solitons & Fractals*, *88*, 38–47.

Buonocore, R. J., Aste, T., & Di Matteo, T. (2017). Asymptotic scaling properties and estimation of the generalized Hurst exponents in financial data. *Physical Review E*, *95*, Article 042311. http://dx.doi.org/10.1103/PhysRevE.95.042311.

Buonocore, R. J., Brandi, G., Mantegna, R. N., & Di Matteo, T. (2019). On the interplay between multiscaling and stock dependence. *Quantitative Finance*, *20*(1), 133–145.

Calvet, L. E., & Fisher, A. J. (2002). Multifractality in asset returns: Theory and evidence. *The Review of Economics and Statistics*, *84*(3), 381–406.

Calvet, L. E., & Fisher, A. J. (2004). How to forecast long-run volatility: Regime switching and the estimation of multifractal processes. *Journal of Financial Econometrics*, *2*(1), 49–83.

Calvet, L. E., Fisher, A. J., & Mandelbrot, B. B. (1997). *Large deviations and the distribution of price changes*: *Cowles Foundation Discussion Papers 1165*, Cowles Foundation for Research in Economics, Yale University.

Carbone, A., Castelli, G., & Stanley, H. E. (2004). Time-dependent Hurst exponent in financial time series. *Physica A: Statistical Mechanics and its Applications*, *344*(1–2), 267–271.

Carling, K. (2000). Resistant outlier rules and the non-Gaussian case. *Computational Statistics & Data Analysis*, *33*(3), 249–258.

Cheridito, P. (2003). Arbitrage in fractional Brownian motion models. *Finance and Stochastics*, *7*(4), 533–553.

Di Matteo, T. (2007). Multi-scaling in finance. *Quantitative Finance*, *7*(1), 21–36.

Di Matteo, T., Aste, T., & Dacorogna, M. M. (2003). Scaling behaviors in differently developed markets. *Physica A: Statistical Mechanics and its Applications*, *324*(1), 183–188.

Di Matteo, T., Aste, T., & Dacorogna, M. M. (2005). Long-term memories of developed and emerging markets: Using the scaling analysis to characterize their stage of development. *Journal of Banking & Finance*, *29*(4), 827–851.

Forde, M., Fukasawa, M., Gerhold, S., & Smith, B. (2022). The Riemann–Liouville field and its GMC as H → 0, and skew flattening for the rough Bergomi model. *Statistics & Probability Letters*, *181*, Article 109265.

Fukasawa, M., Takabatake, T., & Westphal, R. (2019). Is volatility rough? arXiv preprint arXiv:1905.04852.

Gatheral, J., Jaisson, T., & Rosenbaum, M. (2018). Volatility is rough. *Quantitative Finance*, *18*(6), 933–949.

Gençay, R., Dacorogna, M., Muller, U. A., Pictet, O., & Olsen, R. (2001). *An introduction to high-frequency finance*. Elsevier.

Grech, D., & Pamuła, G. (2008). The local Hurst exponent of the financial time series in the vicinity of crashes on the Polish stock exchange market. *Physica A: Statistical Mechanics and its Applications*, *387*(16–17), 4299–4308.

Heber, G., Lunde, A., Shephard, N., & Sheppard, K. (2009). *Oxford-Man Institute's realized library, version 0.3*. Oxford-Man Institute, University of Oxford Oxford.

Heston, S. L. (1993). A closed-form solution for options with stochastic volatility with applications to bond and currency options. *Review of Financial Studies*, *6*(2), 327–343.

Hubert, M., Debruyne, M., & Rousseeuw, P. J. (2018). Minimum covariance determinant and extensions. *Wiley Interdisciplinary Reviews: Computational Statistics*, *10*(3), Article e1421.

[16] A less stringent rule would be to classify as outliers the ones which result in being an outlier for the majority of the specifications rather than for all.

Hurst, H. E. (1956). Methods of using long-term storage in reservoirs.. *Proceedings of the Institution of Civil Engineers*, *5*(5), 519–543.

Jiang, Z.-Q., Xie, W.-J., Zhou, W.-X., & Sornette, D. (2019). Multifractal analysis of financial markets: a review. *Reports on Progress in Physics*, *82*(12), Article 125901.

Kantelhardt, J. W., Zschiegner, S. A., Koscielny-Bunde, E., Havlin, S., Bunde, A., & Stanley, H. E. (2002). Multifractal detrended fluctuation analysis of nonstationary time series. *Physica A: Statistical Mechanics and its Applications*, *316*(1), 87–114.

Kristoufek, L. (2010). Local scaling properties and market turning points at prague stock exchange.. *Acta Physica Polonica B*, *41*(6).

Livieri, G., Mouti, S., Pallavicini, A., & Rosenbaum, M. (2018). Rough volatility: evidence from option prices. *IISE Transactions*, *50*(9), 767–776.

Lux, T. (2004). Detecting multi-fractal properties in asset returns: The failure of the scaling estimator. *International Journal of Modern Physics C*, *15*(04), 481–491. http://dx.doi.org/10.1142/S0129183104005887.

Lux, T., & Marchesi, M. (1999). Scaling and criticality in a stochastic multi-agent model of a financial market. *Nature*, *397*(6719), 498–500.

Mandelbrot, B. B. (1963). The variation of certain speculative prices. *Journal of Business*, *36*(4), 394–419.

Mandelbrot, B. (1967). The variation of some other speculative prices. *Journal of Business*, *40*(4), 393–413.

Mandelbrot, B. B. (1971). When can price be arbitraged efficiently? A limit to the validity of the random walk and martingale models. *The Review of Economics and Statistics*, 225–236.

Mandelbrot, B. (1972). Statistical methodology for nonperiodic cycles: from the covariance to R/S analysis. In *Annals of economic and social measurement, Volume 1, Number 3* (pp. 259–290). NBER.

Mandelbrot, B. B., Fisher, A., & Calvet, L. E. (1997). *A multifractal model of asset returns*: *Cowles Foundation Discussion Papers 1164*, Cowles Foundation for Research in Economics, Yale University.

Mandelbrot, B. B., & Van Ness, J. W. (1968). Fractional Brownian motions, fractional noises and applications. *SIAM Review*, *10*(4), 422–437. http://dx.doi.org/10.1137/1010093.

Mandelbrot, B. B., & Wallis, J. R. (1968). Noah, Joseph, and operational hydrology. *Water Resources Research*, *4*(5), 909–918.

Mantegna, R. N., & Stanley, H. E. (1995). Scaling behaviour in the dynamics of an economic index. *Nature*, *376*(6535), 46–49.

McCrickerd, R., & Pakkanen, M. S. (2018). Turbocharging Monte Carlo pricing for the rough Bergomi model. *Quantitative Finance*, *18*(11), 1877–1886.

Merton, R. C. (1973). Theory of rational option pricing. *The Bell Journal of Economics and Management Science*, 141–183.

Morales, R., Di Matteo, T., Gramatica, R., & Aste, T. (2012). Dynamical generalized Hurst exponent as a tool to monitor unstable periods in financial time series. *Physica A: Statistical Mechanics and its Applications*, *391*(11), 3180–3189.

Pernet, C. R., Wilcox, R. R., & Rousselet, G. A. (2013). Robust correlation analyses: false positive and power validation using a new open source matlab toolbox. *Frontiers in Psychology*, *3*, 606.

Takaishi, T. (2020). Rough volatility of Bitcoin. *Finance Research Letters*, *32*, Article 101379.

Taqqu, M. S. (2013). Benoît mandelbrot and fractional Brownian motion. *Statistical Science*, *28*(1), 131–134.

Wilcox, R. (2004). Inferences based on a skipped correlation coefficient. *Journal of Applied Statistics*, *31*(2), 131–143.

Wilcox, R. R. (2011). *Introduction to robust estimation and hypothesis testing*. Academic Press.

Wilcox, R. R., Rousselet, G. A., & Pernet, C. R. (2018). Improved methods for making inferences about multiple skipped correlations. *Journal of Statistical Computation and Simulation*, *88*(16), 3116–3131.